Molecular Biology of the Cell
Vol. 8, 1129–1142, June 1997

Persistent DNA Damage Inhibits S-Phase and G_2 Progression, and Results in Apoptosis

David K. Orren,* Lone N. Petersen,† and Vilhelm A. Bohr*‡

*Laboratory of Molecular Genetics, National Institute on Aging, National Institutes of Health, Baltimore, Maryland 21224; and †Institute of Molecular Pathology, University of Copenhagen, DK-2100, Copenhagen, Denmark

Submitted January 15, 1997; Accepted March 4, 1997
Monitoring Editor: J. Michael Bishop

We used genetically related Chinese hamster ovary cell lines proficient or deficient in DNA repair to determine the direct role of UV-induced DNA photoproducts in inhibition of DNA replication and in induction of G_2 arrest and apoptosis. UV irradiation of S-phase-synchronized cells causes delays in completion of the S-phase sometimes followed by an extended G_2 arrest and apoptosis. The effects of UV irradiation during the S-phase on subsequent cell cycle progression are magnified in repair-deficient cells, indicating that these effects are initiated by persistent DNA damage and not by direct UV activation of signal transduction pathways. Moreover, among the lesions introduced by UV irradiation, persistence of (6–4) photoproducts inhibits DNA synthesis much more than persistence of cyclobutane pyrimidine dimers (which appear to be efficiently bypassed by the DNA replication apparatus). Apoptosis begins approximately 24 h after UV irradiation of S-phase-synchronized cells, occurs to a greater extent in repair-deficient cells, and correlates well with the inability to escape from an extended late S-phase-G_2 arrest. We also find that nucleotide excision repair activity (including its coupling to transcription) is similar in the S-phase to what we have previously measured in G_1 and G_2.

INTRODUCTION

DNA-damaging agents can have a number of disruptive biological effects on cells. Treatment with certain DNA-damaging agents arrests cell cycle progression by activation of phase-specific checkpoints (reviewed in Hartwell and Weinert, 1989; Murray, 1992; Enoch and Norbury, 1995) or induces the cells to commit suicide by a controlled program known as apoptosis (Lowe *et al.*, 1993a,b; Strasser *et al.*, 1994). G_1, S-phase, and G_2 arrests probably occur by inhibition of the various cyclin-dependent kinase activities that guide cell cycle progression (Lock and Ross, 1990; El-Deiry *et al.*, 1993; O'Connor *et al.*, 1993; Dulic *et al.*, 1994) and putatively allow additional time for the cell to repair DNA damage before replication, during replication, and before mitosis, respectively, thus increasing the fidelity of these processes. However, the exact mechanism by which DNA damage leads to cell cycle arrest remains unknown. In some situations (Lowe *et al.*, 1993a), it is unclear whether cell cycle arrest or apoptosis is induced by DNA damage or by membrane-mediated activation of signal transduction pathways by damaging agents.

On the molecular level, damage in DNA can interfere with transcription, replication, and chromosome segregation. Some lesions in the DNA template strand block elongation of nascent transcripts by eukaryotic RNA polymerases in vitro (Corda *et al.*, 1991; Donahue *et al.*, 1994; Mello *et al.*, 1995). DNA damage can also affect DNA replication, sometimes causing DNA polymerases to misread the template and incorporate the incorrect nucleotide in the daughter strand (Calcagnile *et al.*, 1996). Other types of DNA damage have been shown to block DNA polymerases in vitro (Moore and Strauss, 1979; Moore *et al.*, 1981; Hoffmann *et al.*, 1989), preventing incorporation of any nucleotide in the daughter strand across from the lesion. Polymerase-blocking lesions are thought to result in unreplicated regions in the daughter strand, which might be "re-

‡ Corresponding author: Laboratory of Molecular Genetics, National Institute on Aging, National Institutes of Health, 4940 Eastern Avenue, Baltimore, MD 21224.

paired" by recombinational pathways. Such events might lead to major genetic change such as deletions, insertions, and chromosomal rearrangements. DNA damage, particularly double-strand breaks, may also cause improper chromosome segregation during mitosis, leading to aneuploidy in one or both daughter cells. DNA lesions induced by exposure to UV light are perhaps the most well-studied type of DNA damage. UV irradiation induces almost exclusively two types of adducts between adjacent pyrimidines in DNA: cyclobutane pyrimidine dimers (CPDs;[1] 65–80%) and pyrimidine-pyrimidone (6–4) photoproducts (6–4PPs; 20–35%). Although UV-induced damage inhibits both transcription and replication, the individual contributions of CPDs and 6–4PPs to these effects remains unclear.

A multitude of DNA repair pathways operate to counteract the negative effects of DNA damage. Most bulky helix-distorting lesions, including both CPDs and 6–4PPs, are removed by the nucleotide excision repair (NER) pathway. Many studies (reviewed in Bohr, 1995; Bohr and Anson, 1995) have shown that NER of certain bulky DNA adducts occurs most efficiently in the transcribed strand of active genes, probably through a direct coupling to the transcriptional apparatus (Selby and Sancar, 1993). This transcription-coupled (strand-specific) repair mechanism putatively serves to quickly restore proper gene expression and cellular function. Repair of damage outside of the transcribed strands of active genes is slower but must occur to prevent complications during DNA replication. Obviously, the timing of both the induction of DNA damage and its repair is critical in determining whether lesions are encountered by replication forks during the S-phase.

The genetically related NER-deficient Chinese hamster ovary (CHO) cell lines generated by Busch and co-workers (Busch *et al.*, 1980) provide an ideal system to compare the effects of UV-induced DNA damage on replicative DNA synthesis, cell cycle progression, and apoptosis. The UV5 and UV61 cell lines were directly derived from the AA8 cell line, which has the typical wild-type CHO NER pattern: proficient removal of 6–4PPs from the overall genome and repair of CPDs in the transcribed strand of active genes but not from the rest of the genome (Thompson *et al.*, 1989; Lommel and Hanawalt, 1991; Orren *et al.*, 1996). Even though AA8 cells cannot remove CPDs from inactive areas of their genome, they are still relatively resistant to UV irradiation. The UV5 cell line is mutated in the hamster homologue of the human *XPD* gene (Weber *et al.*, 1988; Flejter *et al.*, 1992), is highly sensitive to UV irradiation, and is completely deficient in repair of both major UV-induced photoproducts (Thompson *et al.*, 1989; Cullinane *et al.*, 1997). The UV61 cell line is mutated in the hamster homologue of the human *CSB* gene (Troelstra *et al.*, 1990; Troelstra *et al.*, 1992), has intermediate UV sensitivity, and appears to be normal in repair of 6–4PPs but deficient in the transcription-coupled repair of CPDs in active genes (Thompson *et al.*, 1989; Lommel and Hanawalt, 1991; Orren *et al.*, 1996). Thus, specific effects of the persistence of each type of UV photoproduct on cell cycle progression can be evaluated by comparing these three cell lines.

Previously, we have shown that UV irradiation of repair-proficient, G_1-, S-, or G_2-synchronized CHO B11 cells delayed progression through the cell cycle (Orren *et al.*, 1995). UV irradiation (20 J/m^2) during mid-S phase resulted in delayed completion of the S-phase followed by an extended (>48 h) G_2 arrest. Apoptosis of a subpopulation of these cells was also noted (Orren *et al.*, 1995). In contrast, irradiation (20 J/m^2) of cells during G_2 caused a relatively brief delay of 4–6 h before passage through mitosis without associated apoptosis. In comparison to these small effects of UV irradiation on G_2-synchronized cells, the heightened effects of UV irradiation on S-phase-synchronized cells suggest that 1) UV-induced DNA damage interferes with the replication process and 2) the action of the replication apparatus on UV-induced photoproducts (and not the UV lesions alone) results in prolonged cell cycle arrest and apoptosis.

In this report, we further investigated the cell cycle progression and apoptotic effects that follow UV irradiation of S-phase-synchronized cells. Both the general effects of UV-induced DNA photoproducts and the specific contributions of both CPDs and 6–4PPs to replication delays, cell cycle arrests, and apoptosis were assessed by use of the CHO cell lines with differing DNA repair capacities. Our results indicate that persistent UV-induced DNA damage (and not activation of signal transduction pathways resulting from general cellular stress) is the cause of prolonged delays in cell cycle progression in both the S-phase and G_2 that eventually lead to apoptosis. Our findings also suggest that the less frequent 6–4PPs are the predominant cause of replication inhibition leading to extended S-G_2 arrest and apoptosis.

MATERIALS AND METHODS

Cell Culture, Synchronization, UV Treatments, and Viability

AA8 cells were obtained from the American Type Culture Collection (Rockville, MD); UV61 and UV5 cells were a kind gift from Drs. D. Busch (Armed Forces Institute of Pathology, Washington DC) and L. Thompson (Lawrence Livermore National Laboratory, Livermore, CA). B11 cells containing an amplification of the *DHFR* gene (Kaufman and Schimke, 1981) were a gift from Dr. L. Chasin (Columbia University, New York, NY). All CHO cells were grown

[1] Abbreviations used: 6–4PP, pyrimidine-pyrimidone (6–4) photoproduct; CHO, Chinese hamster ovary; CPD, cyclobutane pyrimidine dimer; *DHFR*, dihydrofolate reductase; NER, nucleotide excision repair; PBS, phosphate-buffered saline.

in monolayer cultures in a humidified atmosphere of 5% CO_2. AA8, UV61, and UV5 cells were grown in a 1:1 mixture of Ham's F-10 medium (Quality Biological, Gaithersburg, MD) and DMEM (Advanced Biotechnologies Inc., Columbia, MD) supplemented with fetal bovine serum, penicillin (100 U/ml), and streptomycin (100 μg/ml). B11 cells were grown in special F-12 medium (without glycine, hypoxanthine, and thymidine) supplemented with dialyzed fetal bovine serum, penicillin, and streptomycin. Methotrexate (500 nM) was added to maintain selection for amplification of the *DHFR* gene in B11 cells.

Synchronization of all CHO cells was as described previously (Orren *et al.*, 1995), except that a higher concentration of mimosine (100 μM) was used with AA8, UV5, and UV61 cells to prevent passage through the S-phase. Briefly, 1–2 × 10^5 cells were seeded into 100-mm dishes with normal medium (including 10% serum) for about 24 h, then held in low serum (0.2%) medium for at least 48 h to acquire a G_0-G_1 population, and finally released into normal medium containing mimosine for 14 h to allow progression to the beginning of the S-phase (Orren *et al.*, 1995). Although mimosine was originally thought to block the initiation of DNA synthesis, it has recently been shown to inhibit DNA synthesis at a very early stage through depletion of nucleotide pools, similar to hydroxyurea (Gilbert *et al.*, 1995; Hughes and Cook, 1996). After removal of mimosine, cells quickly resume DNA synthesis and proceed synchronously through the S-phase and G_2. Synchronized cells were UV irradiated (254 nm) at 2 or 4 h after removal of mimosine at fluences ranging from 5 to 20 J/m^2. In experiments using mitotic inhibitors, nocodazole (0.1 μg/ml) or colchicine (2.5 μM) was added 4 h after removal of mimosine.

Cell viability after UV treatment was measured using the trypan blue exclusion assay (Freshney, 1987). Briefly, unattached cells were collected by centrifugation (500 × *g*) of medium, resuspended with phosphate-buffered saline (PBS), subjected to centrifugation again, and resuspended in a small volume of PBS. An equal volume of trypan blue solution (0.4% in 0.85% saline, ABI) was added and the viable (unstained) and dead (stained) cells were counted. After the attached cells were dislodged by trypsin treatment and resuspended in medium, cells were prepared for trypan blue treatment and counted as described above for the unattached cells. Percentage of viability was calculated by dividing the number of unstained (attached and unattached) cells by the total number of cells.

Flow Cytometry

The cell cycle phase distributions of unirradiated and irradiated cell populations were determined by flow cytometry as described earlier (Orren *et al.*, 1995). Cells (1–5 × 10^6 cells per sample) were dislodged by trypsin treatment, suspended in normal medium, washed with PBS, and stored in ethanol (70%) at 4°C. On the day of analysis, the cells were treated with RNase and then stained with propidium iodide using materials and instructions from the fluorescence-activated cell sorting kit (Boehringer Mannheim, Indianapolis, IN). Flow cytometry was carried out using a Becton Dickinson FACScan; histograms were generated from which mean fluorescence values and cell cycle phase distributions were calculated with Lysis II and Cellfit software. Fluorescence values significantly below the normal G_1 values are an indication of apoptosis (Nicoletti *et al.*, 1991; Darzynkiewicz *et al.*, 1992). We have not observed a significant contribution of apoptosing G_2 cells to the G_1 or S-phase channels. Apoptosis was independently confirmed with the nucleosomal DNA ladder technique (described below).

Detection of Apoptosis by Gel Electrophoresis

Unattached cells were isolated by centrifugation of medium and suspended together with attached cells removed by trypsin treatment. The combined cells were collected by centrifugation, resuspended in PBS, and pelleted again by centrifugation. The pelleted cells were then lysed by incubation for 16 h at 37°C in a solution of proteinase K (0.5 mg/mL), SDS (17%), Tris (pH 8.0, 0.5 M), EDTA (20 mM), NaCl (10 mM). Total DNA was isolated using the salt extraction technique (Miller *et al.*, 1988). RNA was digested away by treatment with DNase-free RNase (100 μg/ml) for 3 h at 37°C, and the resulting DNA was precipitated and resuspended in TE (10 mM Tris, pH 8.0, 1 mM EDTA) buffer. DNA samples (0.5–1.0 μg) were then electrophoresed on a neutral agarose (0.8%) gel. The gels were stained with ethidium bromide and examined for the presence of nucleosomal-sized fragments indicative of apoptosis (Wyllie, 1980).

Measurement of CPDs in Specific Genes

Measurement of the induction and repair of CPDs in specific DNA sequences was accomplished essentially as described previously (Bohr and Okumoto, 1988). After synchronization in very early S-phase by mimosine treatment (see above), cells were released into normal medium for 2 h then either not irradiated or UV irradiated (10 J/m^2). The cells were lysed immediately or at 18, 36, or 48 h after removal of mimosine. After incubating the lysate for 16 h at 37°C, total DNA was isolated by using the salt extraction procedure and RNase-treated as described above. After ethanol precipitation, DNA was resuspended in TE (0.5–1.0 ml) and digested with *Kpn*I (5 U/μg of DNA) for 3 h at 37°C, yielding a specific 14-kb fragment spanning the first two exons of the hamster *DHFR* gene (Bohr *et al.*, 1986). After another ethanol precipitation, the restricted DNA was resuspended in a minimal volume of TE. Duplicate DNA samples (5 μg each) were either mock treated or treated with T4 endonuclease V for 15 min at 37°C and then electrophoresed in parallel on an alkaline agarose (0.5%) gel for 18 h at 30 V. The DNA was transferred to a nylon membrane with a Posiblot apparatus (Stratagene, La Jolla, CA), then hybridized sequentially with ^{32}P-labeled probes for the transcribed and nontranscribed strands of the hamster *DHFR* gene, described earlier (May *et al.*, 1993). Probes were made using the T7/SP6 transcription kit (Boehringer Mannheim) and [α-^{32}P]CTP (3000 Ci/mmol; ICN, Irvine, CA). After stringency washing, membrane-associated radioactivity was quantitated using a PhosphorImager (Molecular Dynamics, Sunnyvale, CA). The average number of CPDs per 14-kb *DHFR* fragment was determined by comparing the intensity of the T4 endonuclease V-treated sample band with the untreated control using the zero class of the Poisson distribution. Because of the contribution of DNA replicated during the S-phase interval to the total DNA, a decrease of less than half of the initial number of CPDs per fragment was attributed to replication and not repair.

RESULTS

Cell Synchronization

Populations of cells highly synchronized in the S-phase were needed for comparison of the effects of UV irradiation during the S-phase on subsequent cell cycle progression and apoptosis in the AA8, UV61, and UV5 cell lines. As described by Orren *et al.* (1995), we used serum starvation followed by incubation in complete medium plus mimosine to align cells at the beginning of S-phase (Figure 1A). When mimosine is withdrawn, cells proceed synchronously through the remainder of S-phase and then through G_2 and mitosis. This synchronous progression is demonstrated by the gradual increase in DNA content in unirradiated AA8 cells over the 7-h interval after release from mimosine (Figure 1B). At 2, 4, and 6 h after release from mimosine, the cells are in early, mid-, and late S-phase, respectively, and still maintain a high level of syn-

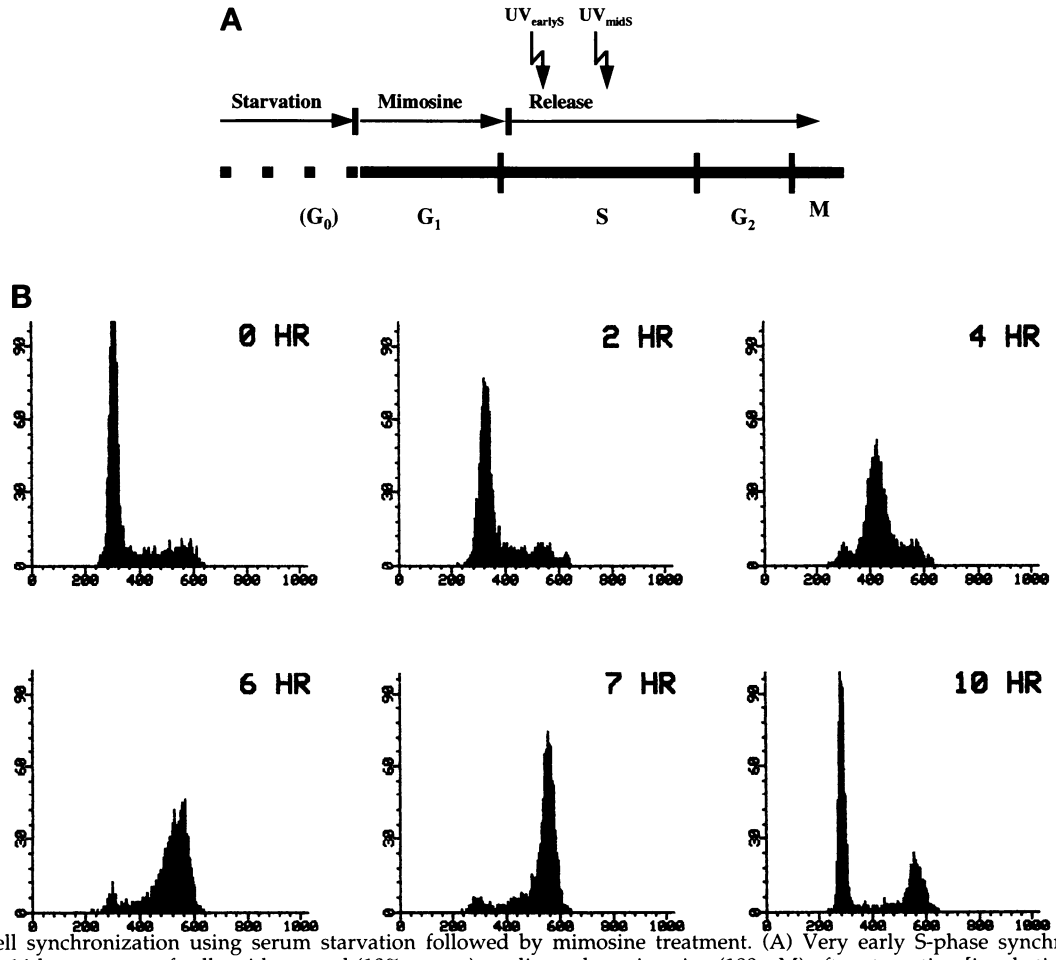

Figure 1. Cell synchronization using serum starvation followed by mimosine treatment. (A) Very early S-phase synchronization was achieved by a 14-h treatment of cells with normal (10% serum) medium plus mimosine (100 μM) after starvation [incubation for >48 h in low serum (0.2%) medium]. After replacement of mimosine-containing medium with normal medium (release), cells traverse the S-phase, G_2, and M. When appropriate, UV irradiations were carried out either 2 (early S-phase) or 4 (mid-S-phase) h after removal of mimosine. (B) AA8 cells were synchronized by the method outlined above and then released from mimosine. Cells were prepared for flow cytometry at 0, 2, 4, 6, 7, and 10 h after removal of mimosine. Histograms were generated from the flow cytometric data; the X-axis and Y-axis represent relative propidium iodide fluorescence (proportional to DNA content) and number of events (cells), respectively.

chrony. By 7 h, almost all of the cells have reached G_2-M and, by 10 h, most have passed through mitosis into the subsequent G_1. The S and G_2-M intervals for unirradiated UV61 and UV5 cells after mimosine release are similar to those of AA8 (see Figure 3A), as are the doubling times (18–20 h) for all three cell lines.

The above procedure was used to obtain highly synchronized cells that, in the experiments described below, were UV irradiated in early or mid-S-phase (2 or 4 h after removal of mimosine, respectively). Cell cycle progression was measured by flow cytometry, which measures the DNA content (via fluorescence) of individual cells. Flow cytometric data are presented in three ways: 1) as histograms (Figures 1B and 4) representing the cell cycle distribution (number of cells with each DNA content) in a single population of cells; 2) as area plots (Figure 2), where changing phase distributions over time are compiled from a series of individual histograms; and 3) as line graphs (Figure 3), where the average DNA content (median fluorescence) in each population at each time point is plotted to emphasize the rate of progression through S-phase.

Effect of UV Dose on Progression of S-Phase-synchronized Repair-proficient Cells

When UV irradiated at a dose of 20 J/m^2 in mid-S-phase, repair-proficient CHO B11 cells undergo a delay in completion of the S-phase followed by an extended G_2 arrest (Orren *et al.*, 1995). In contrast, G_2-irradiated cells undergo only a brief G_2 arrest with no associated apoptosis (Orren *et al.*, 1995). This implies that the action of replication upon UV-induced DNA damage (and not the damage itself) is responsible for the extended G_2 arrest and apoptosis. Initially, this possibility was investigated fur-

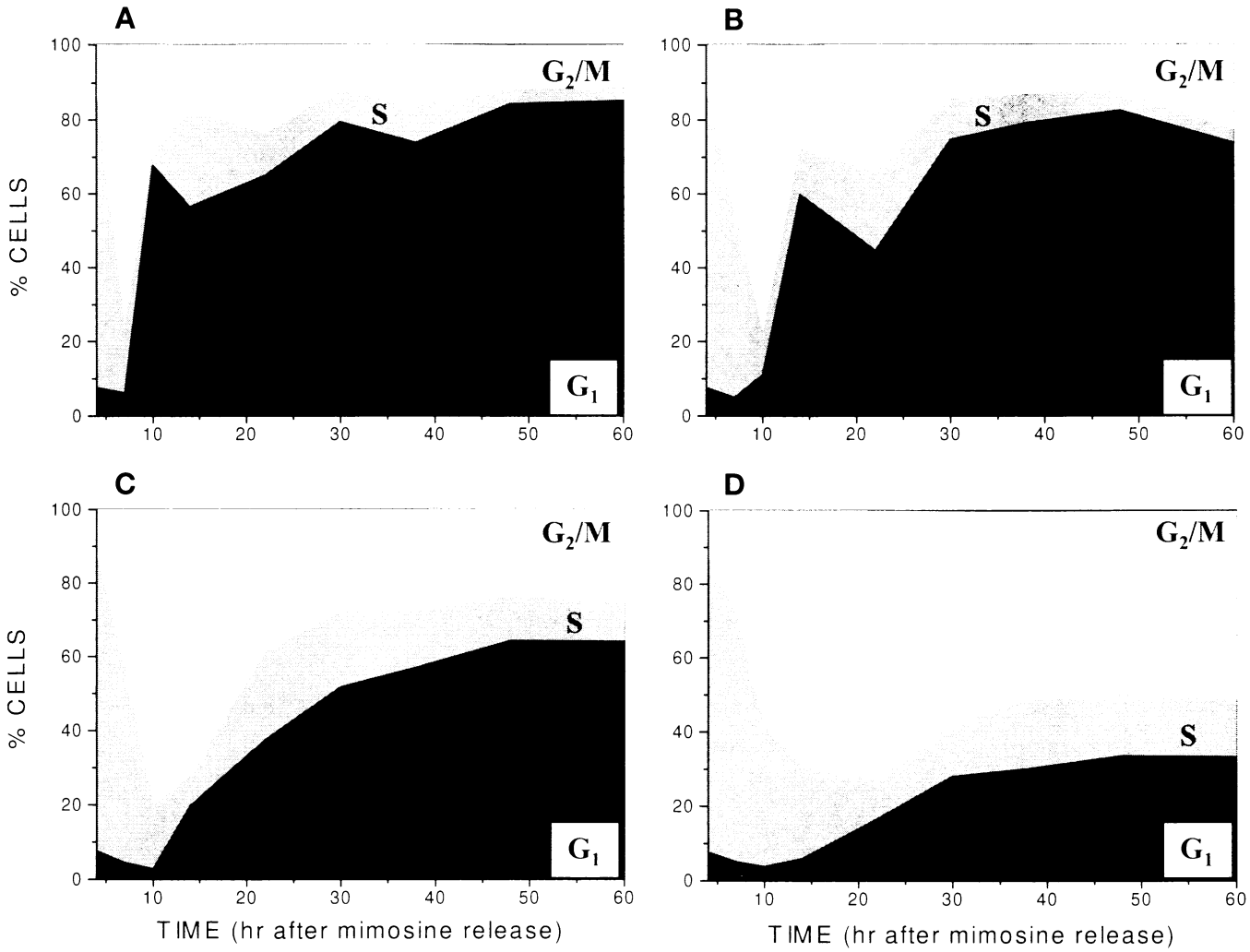

Figure 2. Phase distribution after UV irradiation of mid-S-phase–synchronized AA8 cells. AA8 cells were synchronized by serum deprivation followed by mimosine treatment as described in MATERIALS AND METHODS. At 4 h after removal of mimosine, mid-S-phase–synchronized cells were either not irradiated (A) or UV irradiated at doses of 5 (B), 10 (C), or 15 (D) J/m^2 and then prepared either immediately or after various periods of incubation for flow cytometry. For each time point, the proportions of cells in G_1 (black area), S-phase (dark gray area), and G_2-M (light gray area) were determined by computer analysis of the flow cytometric data. The percentages of cells in each phase over time after irradiation is presented in the form of an area plot.

ther by examining the effect of UV dose on repair-proficient cells after S-phase irradiation. We treated B11 and AA8 cells with various amounts of UV light in mid-S-phase (4 h after mimosine release) and followed their progression by flow cytometry. The percentages of AA8 cells in each cell cycle phase over time after irradiation with 0, 5, 10, or 15 J/m^2 are shown as area plots (Figure 2). Unirradiated cells proceed quickly through S-phase and G_2 and are predominantly in the subsequent G_1 by 12 h after release from mimosine (Figure 2A). After a dose of 5 J/m^2, there is a slight delay in progression through S-phase but essentially no prolonged G_2 arrest, as evidenced by the majority of cells being in G_1 by 16 h after mimosine release (Figure 2B). With higher UV doses, however, progression through S-phase is increasingly slowed (note the increased percentage of S-phase cells between 10 and 15 h in Figure 2, C and D), and the percentages of cells remaining in G_2 for extended periods is increased. After irradiation with doses of 15 J/m^2 (Figure 2D) and above, the majority of AA8 cells remain in G_2 for an extended period (>48 h). B11 cells treated identically have similar cell cycle progression profiles. Thus, in repair-proficient AA8 and B11 cells, inhibition of S-phase progression increases with UV dose, whereas extended G_2 arrest occurs at doses over an approximate threshold of 10–15 J/m^2.

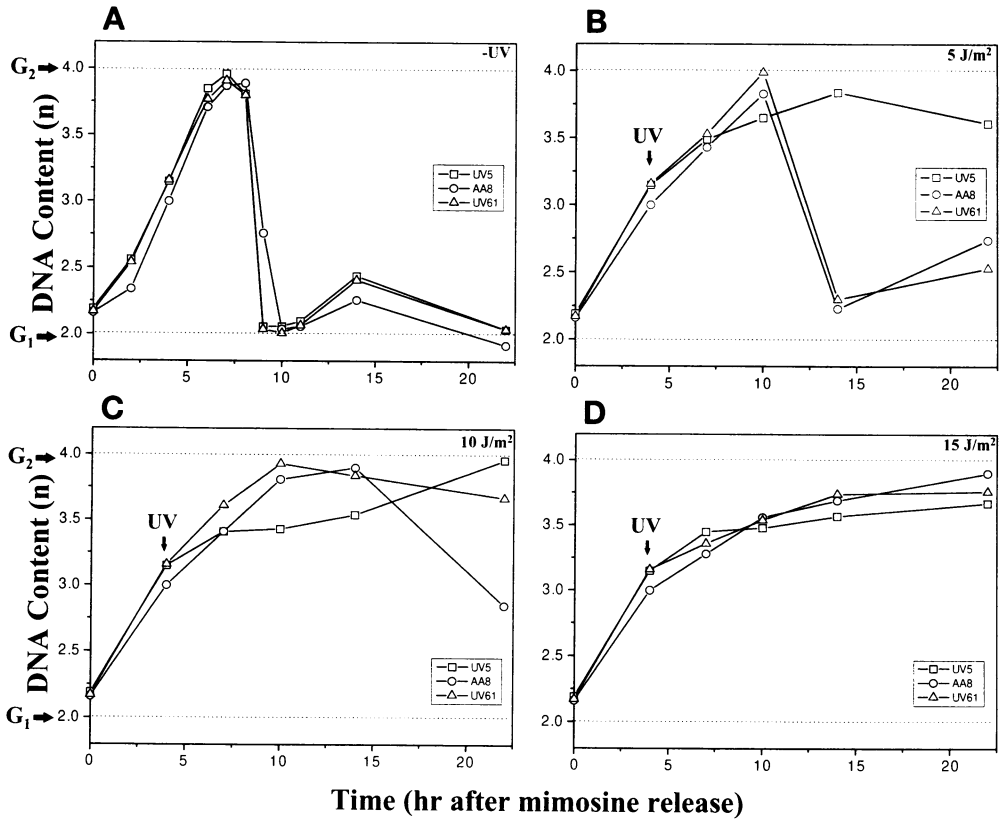

Figure 3. Effect of UV dose on cell cycle progression of mid-S-phase–synchronized AA8, UV61, and UV5 cells. AA8, UV61, and UV5 cells were synchronized by serum deprivation followed by mimosine treatment as described in MATERIALS AND METHODS and then, at 4 h after removal of mimosine, either not treated (A) or UV irradiated at a dose of 5 (B), 10 (C), or 15 (D) J/m^2. Flow cytometric samples were prepared from individual cell populations at the time of release from mimosine (0 h) and at various times after release from mimosine, including the time of UV irradiation (4 h, noted with an arrow in B–D). Median fluorescence values obtained from the flow cytometric data were converted to DNA content values by normalization to a standardized G_2 peak value (4n, upper dotted lines) for each cell line. The G_1 DNA content value (2n, lower dotted line) is assumed to be half of the G_2 peak. The average DNA content values for AA8 (○), UV61 (△), and UV5 (□) cell populations at each UV dose are plotted as a function of time (measured from the point of mimosine release). After the initial increases in DNA content, any significant decrease in DNA content reflects progression of at least part of the population into the subsequent G_1.

Effect of DNA Repair Phenotype on S-Phase Progression and Extended Cell Cycle Arrest

The results presented in Figure 2 cannot distinguish whether the observed effects of UV irradiation on cell cycle progression (and apoptosis) are mediated by DNA damage or by membrane-mediated activation of signal transduction pathways. To elucidate whether DNA damage plays a specific role in the inhibition of DNA replication and extended G_2 arrest, we compared the effects of S-phase irradiation in the parental AA8 cell line (proficient in DNA repair) with those in the UV61 (normal in repair of 6–4PPs but deficient in repair of CPDs in the transcribed strand of active genes) and UV5 (completely defective in repair of both CPDs and 6–4PPs) mutant cell lines. S-phase-synchronized AA8, UV61, and UV5 cells were UV irradiated at 4 h after release from mimosine and their progression was followed by flow cytometry. Figure 3 shows the average DNA content of populations of unirradiated or UV-irradiated (5, 10, or 15 J/m^2) AA8, UV61, and UV5 cells at various times after mimosine release. Because the populations are highly synchronized at the beginning of the S-phase, relative increases in average DNA content after 0 h represent progression through the S-phase toward a maximal (G_2-M) DNA content and significant decreases can be attributed to passage of a proportion of cells through mitosis. With this approach, we can estimate the effect of UV irradiation on both the rate of replication and the ability to pass through mitosis in repair-proficient and -deficient cells. Note that unirradiated AA8, UV61, and UV5 cells have nearly identical rates of progression through S-phase into G_2 and through mitosis (Figure 3A). In contrast, the progression of each cell line through the remainder of the S-phase is delayed at even the lowest dose (5 J/m^2, Figure 3B) and increasingly slowed at higher doses (Figure 3, C and D). The delays are evident by the first time point after UV irradiation and are roughly proportional to the UV dose, suggesting that UV-induced photoproducts directly inhibit replication. A comparison of the different cell lines at each UV dose (Figure 3, B–D) reveals that the delay in completion of S-phase is most pronounced in the completely repair-deficient UV5 cells, and the completion of replication in repair-proficient AA8 and partially repair-deficient UV61 cells is less affected at each dose. In addition, the delays in the attainment of a near-G_2 DNA content after UV irradi-

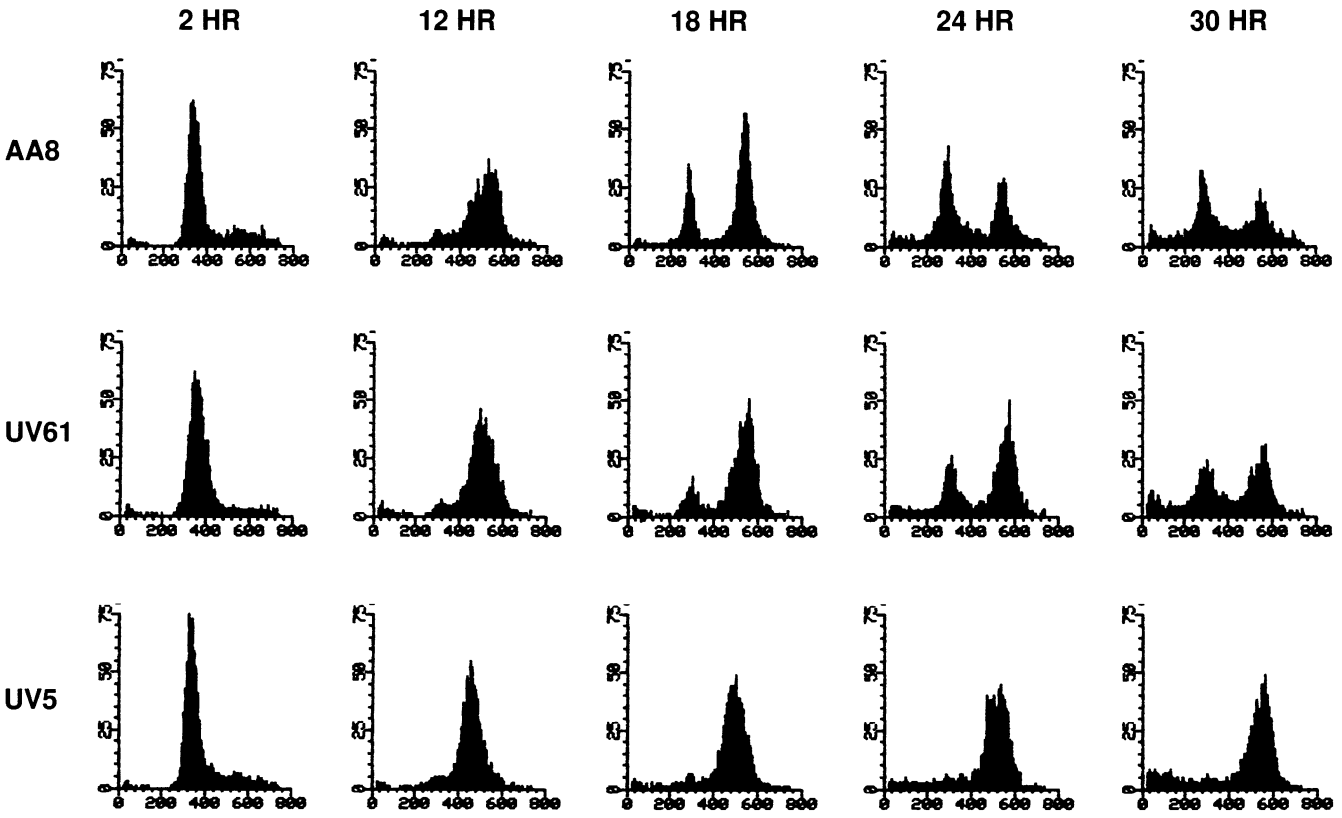

Figure 4. Cell cycle progression of AA8, UV61, and UV5 cells after early S-phase UV irradiation. AA8, UV61, and UV5 cells were synchronized by serum deprivation followed by treatment with mimosine. At 2 h after removal of mimosine, cells were UV irradiated (10 J/m^2) and prepared for flow cytometry either immediately (2-h time point) or after incubation in normal medium until 12, 28, 24, and 30 h after the time of mimosine removal. The flow cytometric data are presented in histogram form as in Figure 1B.

ation are very similar in AA8 and UV61 cells at all doses. However, there are significant differences in the ability of AA8 and UV61 cells to pass through mitosis at equivalent UV doses. Although both cell lines complete the S-phase, G_2, and mitosis with similar kinetics after a UV dose of 5 J/m^2 (Figure 3B), higher doses inhibit mitosis to a greater extent in UV61 cells than in AA8 cells (Figures 3C and 4). In UV5 cells, the ability to pass through mitosis is inhibited even at a UV dose of 5 J/m^2 (Figure 3B). At doses above 10 J/m^2, UV5 cells appear to be unable to even complete replication prior to the loss of cell viability (discussed below). Since the differences in progression between the cell lines were most pronounced at a dose of 10 J/m^2 (and less evident at higher doses), this level of UV irradiation was used for subsequent comparisons.

If the delay in S-phase progression is due to the slowing or blockage of replication fork movement by UV-induced DNA lesions, irradiation earlier in the S-phase will increase the proportion of unreplicated DNA containing UV photoproducts and should amplify any effects of those photoproducts on replication, especially in repair-deficient cells. AA8, UV61, and UV5 cells were irradiated (10 J/m^2) 2 h after release from mimosine, and their cell cycle distributions after various times are shown in histogram form (Figure 4). Unirradiated AA8, UV61, and UV5 cells proceed with normal kinetics through S-phase and enter G_2 approximately 7 h after release from mimosine (Figures 1B and 3A). UV irradiation causes similar delays in progression through the S-phase in both repair-proficient AA8 and partially repair-deficient UV61 cells, with most of the cells having reached G_2 by 18 h (Figure 4). Although a small proportion of AA8 cells remains arrested in G_2 at 30 h, most proceed through mitosis and enter the subsequent G_1. In contrast, a higher proportion of UV61 cells remains arrested in G_2 (Figure 4, compare 24 and 30 h time points). When compared with both AA8 and UV61 cells, irradiated UV5 cells proceed through S-phase at a much slower rate, reaching a near-G_2 state 30 h after release from mimosine. Very few UV5 cells pass through mitosis, with the remainder arrested in late S-phase or G_2. Thus, both early (2 h after mimosine release) and mid-S (4 h after mimosine release) irradiation experiments demonstrate that UV irradiation inhibits replication to a

Table 1. Measurement of CPDs after early S-phase irradiation

Cell line	Strand probed for damage	No. of CPDs/14-kb fragment			
		2 h[a]	18 h	36 h	48 h
AA8	Transcribed	0.53	0.07	0.08	0.03
UV5	Transcribed	0.64	0.44	0.32	N.D.[b]
UV61	Transcribed	0.60	0.34	0.19	0.22
AA8	Nontranscribed	0.73	0.35	0.28	0.27
UV5	Nontranscribed	0.79	0.51	0.44	N.D.
UV61	Nontranscribed	0.68	0.47	0.32	0.28

[a]Time of UV irradiation (10 J/m^2), measured relative to release from mimosine.

[b]N.D., not determined, because of the high percentage of cell dealth in UV5 cells by this time point.

much greater extent in UV5 cells than in either UV61 or AA8 cells. In general, UV irradiation earlier in the S-phase results in longer delays in completion of the S-phase, higher proportions of cells arrested in the S-phase or G_2, and more apoptosis at comparable doses, especially in UV5 cells (Orren and Bohr, unpublished results). When compared with both AA8 and UV61 cells, the more substantial inhibition of S-phase progression in irradiated UV5 cells suggests that unrepaired 6–4PPs inhibit replication to a much greater extent than CPDs. At equivalent UV doses, S-phase progression is delayed to a similar extent in AA8 and UV61 cells, but a higher proportion of UV61 cells undergo a prolonged G_2 arrest.

Induction and Removal of CPDs after S-Phase Irradiation

To adequately compare the effects of UV irradiation on AA8, UV61, and UV5 cells, we had to ensure that equal levels of DNA damage were introduced in the three different cell lines. Therefore, for each cell line, the number of CPDs in an active gene was measured immediately after UV irradiation (10 J/m^2) in early S-phase (2 h after mimosine release). To determine whether repair occurs during S-phase and how it correlates with completion of replication, CPDs were also measured at various intervals after UV irradiation. The number of CPDs in each strand of the *DHFR* gene both initially (2 h) and at 18, 36, and 48 h after release from mimosine is presented in Table 1. There is no substantial difference in the initial level of damage between the AA8, UV61, and UV5 cell lines, although we detect slightly more CPDs in the nontranscribed strand than in the transcribed strand of the *DHFR* gene. Our assay normally measures repair as a reduction in the average number of CPDs per restriction fragment. However, in S-phase–irradiated cells, replication doubles the total pool of DNA fragments by the end of S-phase. Thus, we can conclude that repair occurs only if fewer than half the initial number of CPDs per DNA fragment remain. When this is taken into account, we measured no significant removal of CPDs in the nontranscribed strand in AA8 or in either strand in both UV61 and UV5 (Table 1). In contrast, the removal of CPDs from the transcribed strand in AA8 cells is nearly complete by 18 h, at which time the cells appear to be predominantly in G_2 (Figure 4). However, UV61 cells are also predominantly in G_2 (Figure 4) yet do not repair CPDs by 18 h, suggesting that the lack of CPD repair in the transcribed strand of active genes (in UV61) does not cause additional delays in completion of replication. This also supports the notion that persistent 6–4PPs cause the bulk of the replication delay in UV5 cells and implies that CPDs (in all parts of the genome) are effectively tolerated during replication.

Viability of S-Phase–synchronized Cells after UV Irradiation

Depending upon the UV dose and the repair capacity of the cell, S-phase irradiation also eventually elicited changes in cell cultures consistent with cell death. We measured the timing and amount of cell death in the different cell lines after UV irradiation (0–20 J/m^2) in mid-S-phase (4 h after removal of mimosine), by using the ability of viable cells to exclude trypan blue dye (Figure 5). At each UV dose, quantitatively all of the cells from each cell line exclude trypan blue until 22 h after irradiation. NER-deficient UV5 cells are the most UV sensitive, showing decreased viability (30%) at 60 h at the lowest UV dose (5 J/m^2). At this dose, cell death in UV5 begins by 30 h after mimosine release. At higher doses, the onset of cell death is earlier (by 22 h) and the rate is faster. In contrast, the repair-proficient AA8 cells shows negligible cell death after the lowest UV dose (5 J/m^2). At higher doses, the onset of cell death in AA8 also begins between 22 and 30 h, but the rate and extent of death at each dose are much lower than for UV5 cells. Not surprisingly, the viability of the partially repair-deficient UV61 cells is intermediate between UV5 and AA8 cells. A small proportion of UV61 cells die after a UV dose of 5 J/m^2, which has no effect on AA8 cells and a lethal effect on UV5 cells. At higher doses, most cell death in UV61 occurs somewhat later than in UV5 but by 60 h nearly reaches the same level. In general, the cell viability after UV irradiation roughly reflects the DNA repair capacity of each cell line, although the observed cell death in repair-proficient AA8 cells implies that the repair capacity can be overwhelmed at high UV doses. Interestingly, for each cell line, the onset of cell death corresponds to the beginning of the S-G_2 arrest period and the extent of cell death correlates to the proportions of cells undergoing an extended S-G_2 arrest.

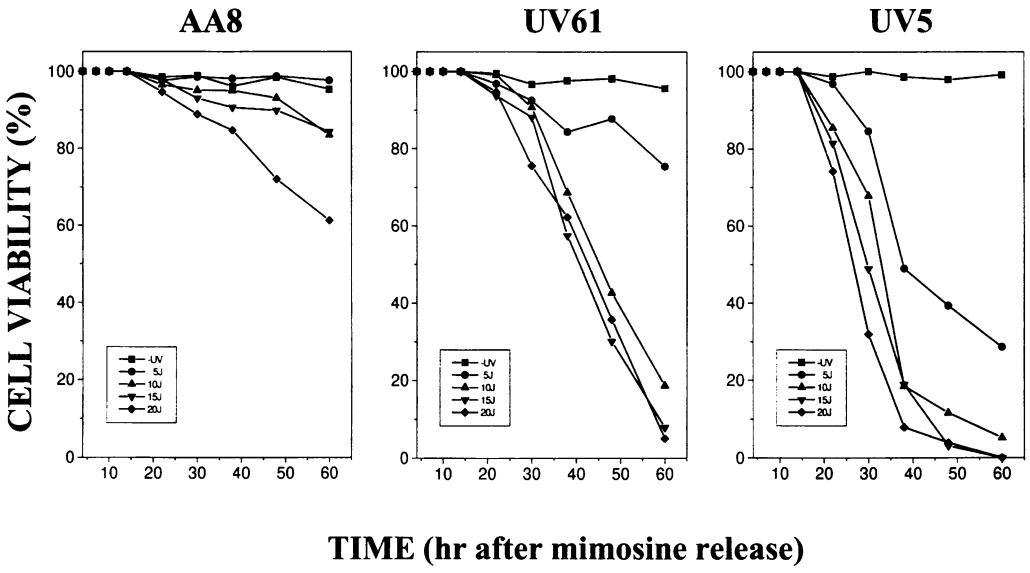

Figure 5. Viability of AA8, UV61, and UV5 cells after S-phase irradiation. AA8, UV61, and UV5 cells were synchronized and not irradiated (■) or UV irradiated with 5 (●), 10 (▲), 15 (▼), or 20 (◆) J/m^2 in mid-S-phase as described in Figure 3. Viability of cells was measured at various times after mimosine release using the trypan blue exclusion assay. Percentage of viability was calculated by dividing the number of cells excluding dye by the total number of cells counted.

Apoptosis after S-Phase UV Irradiation

We wanted to determine whether the UV-induced cell death described above occurs by an apoptotic pathway and whether it correlates specifically with cell cycle arrest caused by persistent DNA damage. After UV irradiation, apoptosis in repair-proficient and -deficient cells was assessed in two ways: 1) by determining the percentage of sub-G_1 fluorescent events in a population of cells analyzed by flow cytometry (Nicoletti *et al.*, 1991; Darzynkiewicz *et al.*, 1992), and 2) by visualizing nucleosomal-sized DNA fragments in purified genomic DNA (Wyllie, 1980). Both assays show that apoptosis is negligible in unirradiated cells (Table 2 and Figure 6, lane 1). Also, in AA8, UV61, and UV5 cells irradiated during G_2, no apoptosis is observed before the subsequent S-phase (Orren and Bohr, unpublished results). In contrast, when cells are irradiated during the S-phase, apoptosis is observed, the extent of which depends upon both the UV dose and

Table 2. Sub-G_1 fluorescence by flow cytometry of AA8, UV61, and UV5 cells irradiated in mid-S-phase

Cell line	UV dose (J/m^2)[a]	% Sub-G_1 fluorescence[b]				
		10 h[a]	22 h	30 h	38 h	48 h
AA8	0	1.2	2.9	1.3	2.3	3.0
	5	3.1	2.2	1.4	2.7	2.6
	10	1.6	3.8	7.8	8.7	9.2
	15	1.4	8.4	13.7	15.7	20.0
	20	2.2	6.2	13.6	15.0	19.8
UV61	0	2.1	1.2	1.6	1.9	2.2
	5	1.4	3.0	10.8	7.6	6.8
	10	2.5	4.6	18.1	26.7	43.0
	15	1.3	3.9	17.9	19.3	51.0
	20	1.2	5.6	14.2	16.2	45.3
UV5	0	1.0	0.8	1.4	1.5	1.3
	5	0.7	2.9	10.6	25.7	26.6
	10	0.5	5.1	13.9	51.1	60.3
	15	1.3	3.3	26.7	20.8	78.5
	20	0.9	6.2	14.7	31.6	81.9

[a]All cell lines were UV irradiated (0–20 J/m^2) 4 h after mimosine release (mid-S-phase) and then prepared for flow cytometry at the times indicated (measured from the point of mimosine release).

[b]Analyzed by flow cytometry, the percentage of total events from a cell population having sub-G_1 fluorescence (DNA content).

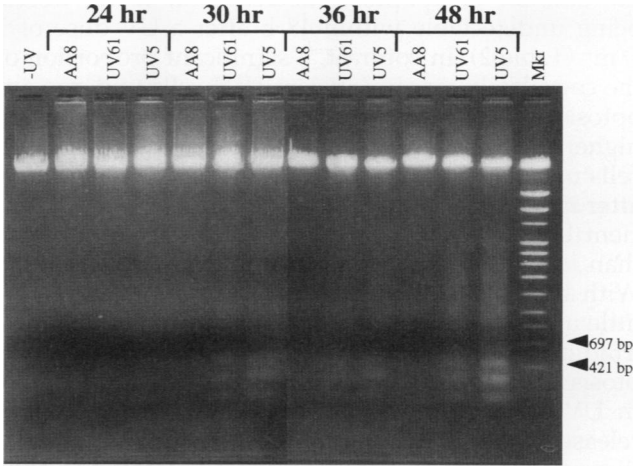

Figure 6. Effect of DNA repair phenotype on apoptotic DNA fragmentation after S-phase irradiation. AA8, UV61, and UV5 cells were synchronized and UV irradiated (10 J/m^2) as described in Figure 4. At 24, 30, 36, and 48 h after removal of mimosine, genomic DNA was isolated from floating and attached cells combined. The DNA was examined for nucleosomal fragmentation by agarose (0.8%) gel electrophoresis with ethidium bromide staining.

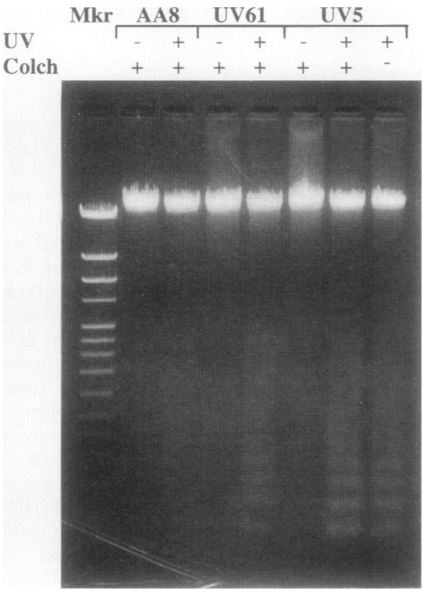

Figure 7. Effect of mitotic inhibitors on apoptotic DNA fragmentation after S-phase irradiation. AA8, UV61, and UV5 cells were synchronized as before, either mock irradiated or UV irradiated (10 J/m^2) in early S-phase (2 h after release from mimosine), and treated with colchicine after 2 h where indicated. At 30 h after mimosine release, genomic DNA was isolated from floating and attached cells combined and analyzed for apoptotic fragments as described in Figure 6.

the repair capacity of each cell line (Table 2 and Figure 6). UV5, UV61, and AA8 cells do not undergo apoptosis until at least 20 h after UV irradiation during S-phase, as measured by the DNA fragmentation assay. AA8 cells undergo apoptosis beginning by 30 h after 20 J/m^2 of UV light delivered in mid-S-phase, but the amount of apoptosis decreases at lower doses, being undetectable within 48 h after a UV dose of 5 J/m^2 (Table 2). In contrast, a significant proportion of the completely repair-deficient UV5 cells undergo apoptosis at a dose of 5 J/m^2, again beginning by 30 h. At higher UV fluences (10–20 J/m^2), nearly all of the UV5 cells undergo apoptosis during the 24- to 48-h period after irradiation (Table 2). In the partially repair-deficient UV61 cells, the extent of apoptosis was greater than in AA8 but less than in UV5 cells at each dose. With the DNA fragmentation assay (Figure 6), very little apoptosis occurs in AA8 over the 48 h after UV irradiation (10 J/m^2) compared with significant apoptosis in both UV61 and UV5. Apoptosis is detectable in UV5 and UV61 by 24 and 30 h after mimosine release, respectively. Our methods recover only a portion of cells that have undergone apoptosis and thus our results probably underestimate the amount of apoptosis. Nevertheless, after S-phase irradiation, losses in cell viability are clearly due to apoptotic cell death, and the extent of apoptosis is roughly proportional to the amount of mitotically arrested cells and is increased in cells (UV5 and UV61) with decreased DNA repair capacity. Combined with the lack of apoptosis after UV irradiation during G_2, these findings suggest that apoptosis results predominantly from persistent DNA damage acted on by replication.

Apoptosis Occurs before Cell Division

Although our results show a correlation between the inability of a cell to pass through cell division and the induction of apoptosis (compare Figures 4 and 6), we could not exclude the possibility that dying cells were actually undergoing mitosis and cytokinesis immediately before apoptosis. To clarify when cells were actually undergoing apoptosis, we again UV-irradiated (10 J/m^2) AA8, UV61, and UV5 cells in early S-phase (2 h after release from mimosine), then added a mitotic inhibitor (either nocodazole or colchicine at 4 h after release from mimosine), subsequently followed cell cycle progression by flow cytometry, and detected apoptosis by the DNA laddering technique. Similar to cells not treated with mitotic inhibitors, the overwhelming proportion of nocodazole- or colchicine-treated UV-irradiated AA8, UV61, or UV5 cells had reached late S-phase or G_2 by 30 h after removal of mimosine. However, irradiated or unirradiated cells treated with nocodazole or colchicine could not divide, as evidenced by the lack of G_1 cells within 48 h (Orren and Bohr, unpublished results). Thus, either nocodazole or colchicine prevented cell division in CHO cells but had no effect on S-phase progression.

Treatment of unirradiated early S-phase–synchronized cells with either nocodazole or colchicine caused a small amount of apoptotic cell death (UV61 > UV5 ≈ AA8), detectable beginning at 30 h after mimosine release. Nevertheless, UV-irradiated (10 J/m^2) cells treated with colchicine undergo much higher levels of apoptosis by 30 h after mimosine release than their unirradiated counterparts (Figure 7). In irradiated cells treated with colchicine, both the onset and extent (Figure 7, lanes 7 and 8) of apoptosis are similar to irradiated untreated cells. Most important, repair-proficient AA8 cells undergo much less irradiation-dependent apoptosis than UV61 and UV5 cells (Figure 7). Similar results were observed with nocodazole. Because treatment with mitotic inhibitors prevented passage into G_1, clearly apoptosis after S-phase irradiation must be occurring from either late S-phase or G_2. Higher UV doses (>10 J/m^2) prevent completion of the S-phase (Figure 3) and induce apoptosis in UV5 cells, indicating that apoptosis can occur from the S-phase.

DISCUSSION

In an earlier study, we observed that UV irradiation of S-phase–synchronized repair-proficient CHO cells initially caused a delay in S-phase progression and then

resulted in an extended G_2 arrest and apoptosis (Orren *et al.*, 1995). Because UV irradiation of cells can result in membrane, protein, and DNA damage, it was unclear which type of damage was responsible for these effects. In fact, UV irradiation causes changes in membrane structure that activate signal transduction pathways (Devary *et al.*, 1992; Engelberg *et al.*, 1994; Sachsenmaier *et al.*, 1994) that could conceivably lead to cell cycle alterations and/or induction of apoptosis. However, our observation that extended G_2 arrest and apoptosis were only associated with UV irradiation during the S-phase (Orren *et al.*, 1995) implies that DNA replication is necessary for these effects. In this report, we determined the contribution of UV-induced DNA damage to inhibition of replication, G_2 arrest, and apoptosis by comparing the effect of S-phase irradiation on genetically related NER-proficient and -deficient CHO cells. Both the UV61 and UV5 cell lines were derived from the parental AA8 cell line, and each has been well characterized with regard to DNA damage sensitivity and DNA repair phenotype (Thompson *et al.*, 1989; Lommel and Hanawalt, 1991; Orren *et al.*, 1996; Cullinane *et al.*, 1997). In the absence of DNA damaging treatments, the three cell lines have the same doubling times and nearly identical S-phase and G_2-M intervals. Our results demonstrate that the same level of UV irradiation (and induced DNA damage) has more pronounced effects on cell cycle progression and eventual apoptosis in two repair-deficient cell lines (UV61 and UV5) than in a repair-proficient cell line (AA8). Moreover, the magnitude of the effects reflects the severity of the DNA repair defect. This evidence indicates that the effects of UV irradiation on cell cycle progression and apoptosis are initiated by persistent DNA damage and not by either the initial number of DNA photoproducts or membrane-mediated alterations in signal transduction pathways.

Previous studies using CHO cells have detected little or no repair of UV-induced CPDs outside the transcribed strand of active genes (Bohr *et al.*, 1985; Mellon *et al.*, 1987; May *et al.*, 1993). However, in those studies replicated DNA was removed prior to detection of damage, thus eliminating the contribution of damage (and repair) in replicated DNA. Our experiments extend the earlier findings by measuring gene-specific CPD removal in replicated and unreplicated DNA during S-phase. Consistent with other repair measurements in asynchronous cells (Thompson *et al.*, 1989; Cullinane *et al.*, 1996; Orren *et al.*, 1996), no significant removal of CPDs in either UV5 or UV61 could be detected after early S-phase irradiation. In contrast, CPDs were almost completely removed from the transcribed strand of the *DHFR* gene by 16 h after irradiation of early S-phase–synchronized AA8 cells but not detectably removed from the nontranscribed strand. Our results indicate that CPD repair activity during ongoing replication is similar to that in asynchronous cells (Bohr *et al.*, 1985; Mellon *et al.*, 1987; May *et al.*, 1993) and in G_1 and G_2 (Lommel *et al.*, 1995; Petersen *et al.*, 1995). Repair of 6–4PPs is also constant throughout the cell cycle (Mitchell *et al.*, 1995). Thus, in repair-proficient AA8 and B11 CHO cells, 6–4PPs are constantly and quickly removed from the entire genome but CPDs are only removed from the transcribed strand of active genes. Persistent base damage in nontranscribed regions of the genome would not be expected to inhibit transcription; however, distorting base damage in DNA would be expected to disrupt replication, in which both strands of the entire genome are used as templates. Since CHO cells cannot remove CPDs from inactive DNA by NER, they must have another mechanism to tolerate this specific type of damage.

The fact that ongoing replication neither inhibits nor enhances DNA repair activity allowed us to examine the effect of UV photoproducts on replication. Most of the earlier studies measuring the effect of UV irradiation on replication simply document a reduction in the rate of incorporation of nucleotides into newly synthesized DNA from asynchronous cells, which might occur by numerous mechanisms, including cell cycle arrest, inhibition of replicon initiation, or blockage of replication fork movement. Our studies have two major advantages compared with earlier reports. First, we are investigating the effect of UV irradiation on cells highly synchronized during the S-phase, thus eliminating any nonreplication specific effects (such as G_1 and/or G_2 arrest) that could inhibit DNA synthesis. Second, by using cell lines with varying NER capacity, we can compare the individual contributions of the major UV photoproducts (and their repair) to inhibition of DNA replication. Specifically, UV5 cells cannot repair either 6–4PPs or CPDs (Thompson *et al.*, 1989; Cullinane *et al.*, 1996), UV61 cells repair 6–4PPs normally but are defective in the transcription-coupled repair of CPDs (Thompson *et al.*, 1989; Lommel and Hanawalt, 1991; Orren *et al.*, 1996), and AA8 cells repair 6–4PPs normally and CPDs in transcribed strands of active genes (Thompson *et al.*, 1989; Lommel and Hanawalt, 1991; Orren *et al.*, 1996). Our comparison of the effect of UV irradiation and DNA repair capacity on replication is facilitated by the finding that both the S-phase intervals in unirradiated cells and the amount of DNA damage induced at each UV dose are equivalent in the three cell lines. In each cell line, S-phase progression slows with increasing UV dose, implying that additional DNA damage increasingly inhibits ongoing replication. Comparable UV doses inhibit the rate of replication similarly in AA8 and UV61 but much more severely in UV5. Moreover, UV5 cells have difficulty attaining a G_2 (4n) content of DNA after S-phase irradiation with doses greater than 10 J/m^2. Considering the inability of UV5 cells to remove 6–4PPs from DNA (in comparison to the normal

6–4PP repair by AA8 and UV61), this evidence strongly suggests that the less frequent 6–4PPs inhibit replication to a much greater extent than CPDs. Since replication (and putatively activation of late-firing replicons) is resumed and completed in AA8 and UV61 cells that are subject to the same UV dose, this inhibition is most likely due to a direct effect of 6–4PPs on replication elongation. Although we cannot rule out the specific inhibition of late-firing replicons by persistent 6–4PPs, we speculate that DNA polymerases cannot synthesize past a 6–4PP in the template, effectively blocking replication fork movement. This may result in unreplicated regions in the vicinity of 6–4PPs, potentially leading to chromosomal aberrations. This may explain the S-phase–dependent clastogenic effects of UV irradiation (Kaufmann and Wilson, 1994). The shorter delays in completion of S-phase in AA8 and UV61 cells may be due to the interval required for removal of 6–4PPs and/or pausing of replication forks at CPD sites. It has been suggested that the bulk of replication inhibition in mammalian cells is caused by 6–4PPs (Cleaver *et al.*, 1987; Taft *et al.*, 1991), but still considerable controversy exists concerning the relative contributions of each photoproduct. Although some studies have shown that CPDs block DNA polymerases in vitro (Moore and Strauss, 1979; Moore *et al.*, 1981) and in vivo on simian virus 40 replication forks (Berger and Edenberg, 1986), the fact that CHO cells that do not repair CPDs in nontranscribed regions can complete replication and mitosis after significant UV doses indicates that DNA polymerase complexes can synthesize past CPDs in the template. Translesion synthesis of CPDs by eukaryotic DNA polymerases has been demonstrated in vitro (O'Day *et al.*, 1992; Thomas and Kunkel, 1993) and was suggested to explain the persistence of CPDs in the parental strands of replicated DNA from CHO cells (Spivak and Hanawalt, 1992).

Our results clearly and consistently demonstrate extended cell cycle arrest and apoptosis after UV irradiation of S-phase–synchronized cells. In contrast, cells (repair-proficient and -deficient) irradiated during G_2 only undergo a brief arrest before mitosis and do not undergo apoptosis before the subsequent S-phase (Orren *et al.*, 1995; Orren and Bohr, unpublished data). This relative insensitivity of G_2 cells indicates that the UV-induced DNA photoproducts do not directly cause extended arrest or apoptosis, whereas the dramatic sensitivity of S-phase cells suggests that the action of replication on UV photoproducts results in extended arrest and apoptosis. Our results show that both UV5 and UV61 cells undergo this extended arrest at lower UV doses than do AA8 cells and confirm that persistent DNA damage present during S-phase is the major causative factor. The significant G_2 arrest and apoptosis in repair-proficient AA8 cells at high UV doses (15 J/m^2 and above) suggest that high levels of damage can overwhelm the ability of repair mechanisms to remove lesions (perhaps the critical 6–4PPs) prior to passage of replication forks (Orren *et al.*, 1995; this study). The extent of apoptosis in each cell type at a given UV dose correlates with the proportions of cells arrested before mitosis. Apoptosis begins approximately 24 h after S-phase irradiation and occurs from either S-phase (in the case of UV5 cells after UV doses above 10 J/m^2) or G_2. As detailed above, 6–4PPs are more effective than CPDs at blocking replication, a fact that, therefore, probably explains the increased incidence of S-G_2 arrest and apoptosis in UV5 (in comparison to UV61) at low UV doses. However, after irradiation in S-phase with comparable UV doses, UV61 cells do undergo G_2 arrest and apoptosis to a greater degree than AA8 cells, implying that a defect in transcription-coupled repair has some contribution to this effect. Possible explanations for this are: 1) 6–4PP removal from transcribed strands of active genes is inhibited in UV61, resulting in more unreplicated regions; 2) persistence of CPDs in the transcribed strands of active genes inhibits transcription essential for the cell to pass through mitosis; or 3) persistence of 6–4PPs or CPDs in transcribed strands directly signals cell cycle arrest and apoptotic pathways. Recent reports show that persistence of damage in the transcribed strand of active genes correlates with stabilization of p53 protein and apoptosis (Yamaizumi and Sugano, 1994; Ljungman and Zhang, 1996). However, because CHO cells have constitutively stable mutated p53 protein (Orren *et al.*, 1995), its participation in any cell cycle arrest or apoptotic pathway is questionable.

The S-phase dependence of both extended arrest and apoptosis is consistent with a model in which 1) persistent DNA damage prevents the accurate completion of replication, which, in turn, relays a signal that prevents the cell from entering mitosis and 2) inability to repair the replication-induced damage over time triggers p53-independent apoptosis. This model is supported by the facts that checkpoint pathways that monitor replication and its accurate completion and prevent mitosis have been found in yeast (Navas *et al.*, 1995; Paulovich and Hartwell, 1995) and p53-independent apoptosis from G_2-M after cisplatin treatment has been observed in immortalized human B cells (Allday *et al.*, 1995).

We have demonstrated that persistent UV-induced DNA damage inhibits replication directly, subsequently activating cell cycle arrest and apoptotic pathways. These effects are probably triggered by unreplicated regions in the vicinity of UV photoproducts in the template strand, as base damage alone induced during G_2 does not cause cell cycle arrest and apoptosis (Orren *et al.*, 1995). This replication-mediated pathway enhances the toxicity of DNA damaging agents and may be a general mechanism by which cells con-

taining severe and unrepairable DNA damage are removed from a population.

ACKNOWLEDGMENTS

We thank Robert Pyle, Irina Dianova, Signe Skjoldager, and Lata Prabhakar for technical assistance and Drs. Leonora Lipinski and A.S. Balajee for critical reading of the manuscript. We are also grateful for interactions with the Danish Center for Molecular Gerontology.

REFERENCES

Allday, M.J., Inman, G.J., Crawford, D.H., and Farrell, P.J. (1995). DNA damage in human B cells can induce apoptosis, proceeding from G1/S when p53 is transactivation competent and G2/M when it is transactivation defective. EMBO J. *14*, 4994–5005.

Berger, C.A., and Edenberg, H.J. (1986). Pyrimidine dimers block simian virus 40 replication forks. Mol. Cell. Biol. *6*, 3443–3450.

Bohr, V. (1995). DNA repair fine structure and its relations to genomic instability. Carcinogenesis *16*, 2885–2892.

Bohr, V., and Anson, R. (1995). DNA damage, mutation and fine structure DNA repair in aging. Mutat. Res. *338*, 25–34.

Bohr, V., and Okumoto, D.S. (1988). Analysis of pyrimidine dimers in defined genes. In: A Laboratory Manual of Research Procedures, ed. E. Friedberg and P. Hanawalt, New York: Marcel Dekker, 347–366.

Bohr, V.A., Okumoto, D.S., Ho, L., and Hanawalt, P.C. (1986). Characterization of a DNA repair domain containing the dihydrofolate reductase gene in Chinese hamster ovary cells. J. Biol. Chem. *261*, 16666–16672.

Bohr, V., Smith, C., Okumoto, D.S., and Hanawalt, P. (1985). DNA repair in an active gene: removal of pyrimidine dimers from the *DHFR* gene of CHO cells is much more efficient than in the genome overall. Cell *40*, 359–369.

Busch, D., Cleaver, J., and Gasser, D. (1980). Large-scale isolation of UV-sensitive clones of CHO cells. Somatic Cell Genet. *6*, 407–418.

Calcagnile, A., Basic-Zaninovic, T., Palombo, F., and Dogliotti, E. (1996). Misincorporation rate and type on the leading and lagging strands of UV-damaged DNA. Nucleic Acids Res. *24*, 3005–3009.

Cleaver, J.E., Cortes, F., Lutze, L.H., Morgan, W.F., Player, A.N., and Mitchell, D.L. (1987). Unique DNA repair properties of a xeroderma pigmentosum revertant. Mol. Cell. Biol. *7*, 3353–3357.

Corda, Y., Job, C., Anin, M.-F., Leng, M., and Job, D. (1991). Transcription by eucaryotic and procaryotic RNA polymerases of DNA modified at a d(GG) or a d(AG) site by the antitumor drug *cis*-diamminedichloroplatinum(II). Biochemistry *30*, 222–230.

Cullinane, C., Weber, C.A., Dianov, G., and Bohr, V.A. (1997). Restoration of preferential and strand specific repair in group 2 CHO mutants (UV5) by the *XPD* (*ERCC2*) gene. Carcinogenesis (*in press*).

Darzynkiewicz, Z., Bruno, S., Del Bino, G., Gorczyca, W., Hotz, M.A., Lassota, P., and Traganos, F. (1992). Features of apoptotic cells measured by flow cytometry. Cytometry *13*, 795–808.

Devary, Y., Gottlieb, R.A., Smeal, T., and Karin, M. (1992). The mammalian ultraviolet response is triggered by activation of Src tyrosine kinases. Cell *71*, 1081–1091.

Donahue, B.A., Yin, S., Taylor, J.-S., Reines, D., and Hanawalt, P.C. (1994). Transcript cleavage by RNA polymerase II arrested by a cyclobutane pyrimidine dimer in the DNA template. Proc. Natl. Acad. Sci. USA *91*, 8502–8506.

Dulic, V., Kaufmann, W.K., Wilson, S., Tlsty, T., Lees, E., Harper, J.W., Elledge, S.J., and Reed, S.I. (1994). p53-dependent inhibition of cyclin dependent kinase activities in human fibroblasts during radiation-induced G1 arrest. Cell *76*, 1013–1023.

El-Deiry, W.S., Tokino, T., Velculescu, V.E., Levy, D.B., Parsons, R., Trent, J.M., Lin, D., Mercer, W.E., Kinzler, K.W., and Vogelstein, B. (1993). WAF1, a potential mediator of p53 tumor suppression. Cell *75*, 817–825.

Engelberg, D., Klein, C., Martinetto, H., Struhl, K., and Karin, M. (1994). The UV response involving the Ras signaling pathway and AP-1 transcription factors is conserved between yeast and mammals. Cell *77*, 381–390.

Enoch, T., and Norbury, C. (1995). Cellular responses to DNA damage: cell cycle checkpoints, apoptosis, and the roles of p53 and ATM. Trends Biochem. Sci. *20*, 426–430.

Flejter, W.L., McDaniel, L.D., Johns, D., Friedberg, E.C., and Schultz, R.A. (1992). Correction of xeroderma pigmentosum complementation group D mutant cell phenotypes by chromosome and gene transfer: involvement of the human *ERCC2* DNA repair gene. Proc. Natl. Acad. Sci. USA *89*, 261–265.

Freshney, R.I. (1987). Measurement of cytotoxicity and viability. Culture of Animal Cells: A Manual of Basic Technique, New York: Alan R. Liss, 245–256.

Gilbert, D.M., Neilson, A., Miyazawa, H., DePamphilis, M.L., and Burhans, W.C. (1995). Mimosine arrests DNA synthesis at replication forks by inhibiting deoxyribonucleotide metabolism. J. Biol. Chem. *270*, 9597–9606.

Hartwell, L.H., and Weinert, T.A. (1989). Checkpoints: controls that ensure the order of cell cycle events. Science *246*, 629–634.

Hoffmann, J.-S., Johnson, N.P., and Villani, G. (1989). Conversion of monofunctional DNA adducts of *cis*-diamminedichloroplatinum(II) to bifunctional lesions. J. Biol. Chem. *264*, 15130–15135.

Hughes, T.A., and Cook, P.R. (1996). Mimosine arrests the cell cycle after cells enter S-phase. Exp. Cell Res. *222*, 275–280.

Kaufman, R.J., and Schimke, R.T. (1981). Amplification and loss of dihydrofolate reductase genes in a Chinese hamster ovary cell line. Mol. Cell. Biol. *1*, 1069–1076.

Kaufmann, W.K., and Wilson, S.J. (1994). G_1 arrest and cell-cycle-dependent clastogenesis in UV-irradiated human fibroblasts. Mutat. Res. *314*, 67–76.

Ljungman, M., and Zhang, F. (1996). Blockage of RNA polymerase as a possible trigger for u.v. light-induced apoptosis. Oncogene *13*, 823–831.

Lock, R.B., and Ross, W.E. (1990). Inhibition of $p34^{cdc2}$ kinase activity by etoposide or irradiation as a mechanism of G_2 arrest in Chinese hamster ovary cells. Cancer Res. *50*, 3761–3766.

Lommel, L., Carswell-Crumpton, C., and Hanawalt, P.C. (1995). Preferential repair of the transcribed DNA strand in the dihydrofolate reductase gene throughout the cell cycle in UV-irradiated human cells. Mutat. Res. *336*, 181–192.

Lommel, L., and Hanawalt, P. (1991). The genetic defect in the Chinese hamster ovary cell mutant UV61 permits moderate selective repair of cyclobutane pyrimidine dimers in an expressed gene. Mutat. Res. *255*, 183–191.

Lowe, S.W., Ruley, H.E., Jacks, T., and Housman, D.E. (1993a). p53-dependent apoptosis modulates the cytotoxicity of anticancer agents. Cell *74*, 957–967.

Lowe, S.W., Schmitt, E.M., Smith, S.W., Osborne, B.A., and Jacks, T. (1993b). p53 is required for radiation-induced apoptosis in mouse thymocytes. Nature *362*, 847–849.

May, A., Nairn, R.S., Okumoto, D.S., Wassermann, K., Stevnsner, T., and Jones, J.C. (1993). Repair of individual DNA strands in the hamster dihydrofolate reductase gene after treatment with ultraviolet light, alkylating agents, and cisplatin. J. Biol. Chem. *268*, 1650–1657.

Mello, J.A., Lippard, S.J., and Essigmann, J.M. (1995). DNA adducts of cis-diaminedichloroplatinum(II) and its trans isomer inhibit RNA polymerase II differentially in vivo. Biochemistry *34*, 14783–14791.

Mellon, I., Spivak, G., and Hanawalt, P.C. (1987). Selective removal of transcription-blocking DNA damage from the transcribed strand of the mammalian *DHFR* gene. Cell *51*, 241–249.

Miller, S.A., Dykes, D.D., and Polesky, H.F. (1988). A simple salting out procedure for extracting DNA from human nucleated cells. Nucleic Acids Res. *16*, 1215.

Mitchell, D.L., Cleaver, J.E., Lowery, M.P., and Hewitt, R.R. (1995). Induction and repair of (6–4) photoproducts in normal human and xeroderma pigmentosum variant cells during the cell cycle. Mutat. Res. *337*, 161–167.

Moore, P.D., Bose, K.K., Rabkin, S.D., and Strauss, B.S. (1981). Sites of termination of in vitro DNA synthesis on ultraviolet- and N-acetylaminofluorene-treated ϕX174 templates by prokaryotic and eukaryotic DNA polymerases. Proc. Natl. Acad. Sci. USA *78*, 110–114.

Moore, P., and Strauss, B.S. (1979). Sites of inhibition of in vitro DNA synthesis in carcinogen- and UV-treated ϕX174 DNA. Nature *278*, 664–666.

Murray, A. (1992). Creative blocks: cell-cycle checkpoints and feedback controls. Nature *359*, 599–604.

Navas, T.A., Zhou, Z., and Elledge, S.J. (1995). DNA polymerase ϵ links the DNA replication machinery to the S phase checkpoint. Cell *80*, 29–39.

Nicoletti, I., Migliorati, G., Pagliacci, M.C., Grignani, F., and Riccardi, C. (1991). A rapid and simple method for measuring thymocyte apoptosis by propidium iodide staining and flow cytometry. J. Immunol. Methods *139*, 271–279.

O'Connor, P.M., Ferris, D.K., Pagano, M., Draetta, G., Pines, J., Hunter, T., Longo, D.L., and Kohn, K.W. (1993). G_2 delay induced by nitrogen mustard in human cells affects cyclin A/cdk2 and cyclin B/cdc2-kinase complexes differently. J. Biol. Chem. *268*, 8298–8308.

O'Day, C.L., Burgers, P.M.J., and Taylor, J.-S. (1992). PCNA-induced DNA synthesis past cis-syn and trans-syn-I thymine dimers by calf thymus DNA polymerase δ in vitro. Nucleic Acids Res. *20*, 5403–5406.

Orren, D.K., Dianov, G., and Bohr, V.A. (1996). The human *CSB* (*ERCC6*) gene corrects the transcription-coupled repair defect in the CHO cell mutant UV61. Nucleic Acids Res. *24*, 3317–3323.

Orren, D.K., Petersen, L.N., and Bohr, V.A. (1995). A UV-responsive G_2 checkpoint in rodent cells. Mol. Cell. Biol. *15*, 3722–3730.

Paulovich, A.G., and Hartwell, L.H. (1995). A checkpoint regulates the rate of progression through S phase in *S. cerevisiae* in response to DNA damage. Cell *82*, 841–847.

Petersen, L.N., Orren, D.K., and Bohr, V.A. (1995). Gene-specific and strand-specific DNA repair in the G_1 and G_2 phases of the cell cycle. Mol. Cell. Biol. *15*, 3731–3737.

Sachsenmaier, C., Radler-Pohl, A., Zinck, R., Nordheim, A., Herrlich, P., and Rahmsdorf, H.J. (1994). Involvement of growth factor receptors in the mammalian UVC response. Cell *78*, 963–972.

Selby, C.P., and Sancar, A. (1993). Molecular mechanism of transcription-repair coupling. Science *260*, 53–58.

Spivak, G., and Hanawalt, P.C. (1992). Translesion DNA synthesis in the dihydrofolate reductase domain of UV-irradiated CHO cells. Biochemistry *31*, 6794–6800.

Strasser, A., Harris, A.W., Jacks, T., and Cory, S. (1994). DNA damage can induce apoptosis in proliferating lymphoid cells via p53-independent mechanisms inhibitable by Bcl-2. Cell *79*, 329–339.

Taft, S.A., Ling, S.Y., and Griffiths, T.D. (1991). Effect of UV light on sister-chromatid exchanges, activation of alternative sites of replicon initiation and thymidine incorporation in CHO AA8, UV61 and UV5 cells. Mutat. Res. *255*, 257–264.

Thomas, D.C., and Kunkel, T.A. (1993). Replication of UV-irradiated DNA in human cell extracts: evidence for mutagenic bypass of pyrimidine dimers. Proc. Natl. Acad. Sci. USA *90*, 7744–7748.

Thompson, L., Mitchell, D., Regan, J., Bouffler, S., Stewart, S., Carrier, W., Nairn, R., and Johnson, R. (1989). CHO mutant UV61 removes (6–4) photoproducts but not cyclobutane dimers. Mutagenesis *4*, 140–146.

Troelstra, C., Odijk, H., de Wit, J., Westerveld, A., Thompson, L., Bootsma, D., and Hoeijmakers, J. (1990). Molecular cloning of the human DNA excision repair gene *ERCC-6*. Mol. Cell. Biol. *10*, 5806–5813.

Troelstra, C., van Gool, A., de Witt, J., Vermeulen, W., Bootsma, D., and Hoeijmakers, J.H.J. (1992). ERCC6, a member of a subfamily of putative helicases, is involved in Cockayne's syndrome and preferential repair of active genes. Cell *71*, 939–953.

Weber, C.A., Salazar, E.P., Stewart, S.A., and Thompson, L.H. (1988). Molecular cloning and biological characterization of a human gene, *ERCC2*, that corrects the nucleotide excision repair defect in CHO UV5 cells. Mol. Cell. Biol. *8*, 1137–1146.

Wyllie, A.H. (1980). Glucocorticoid-induced thymocyte apoptosis is associated with endogenous endonuclease activation. Nature *284*, 555–556.

Yamaizumi, M., and Sugano, T. (1994). UV-induced nuclear accumulation of p53 is evoked through DNA damage of actively transcribed genes independent of the cell cycle. Oncogene *9*, 2775–2784.